

TURBULENCE IN THE SOLAR PHOTOSPHERE

K. Petrovay

*Eötvös University, Dept. of Astronomy, Budapest, Pf. 32, H-1518 Hungary, and
Instituto de Astrofísica de Canarias, La Laguna, Tenerife, E-38200 Spain*

[*Space Science Reviews*, **95**, 9–24 (2001)]

Abstract. The precise nature of photospheric flows, and of the transport effects they give rise to, has been the subject of intense debate in the last decade. Here we attempt to give a brief review of the subject emphasizing interdisciplinary (solar physics—turbulence theory) aspects, key open questions, and recent developments.

1. Introduction

The stochastic nature of the motions observed on the Sun and their enormous Reynolds numbers suggest that the photospheric plasma must be in a strongly turbulent state. On the other hand, the extreme physical conditions prevailing in the photosphere (strong inhomogeneity and anisotropy, non-diffusive radiative transfer, penetrative convective motions in a stably stratified layer, compressibility effects, intermittency, etc.) imply that photospheric motions differ fundamentally from the textbook case of isotropic incompressible Kolmogorov turbulence. The precise nature of these flows, and of the transport effects they give rise to, has been the subject of intense debate in the last decade. The contradictory views formulated on the topic range from naïve and uncritical applications of the Kolmogorov theory to the outright denial of the turbulent nature of photospheric flows.

The aim of this paper is not to give an exhaustive review or to cite all relevant papers. Instead, the emphasis will be on interdisciplinary aspects, key open questions, and recent developments.

2. The nature of photospheric flows

2.1. MHD TURBULENCE: A SUMMARY OF THEORY AND EXPERIMENTS

2.1.1. *Phenomenology: shear instability, cascade, inertial range*

In a very simplistic description that still grasps the essence, turbulence may be regarded as the result of shear flow instability. Shear instabilities are present in a very wide class of flows. In the nonlinear regime the unstable modes develop into vortices with characteristic scales similar to the length scale L of the shear of the original velocity field. The instability develops on a timescale L/V , V being the scale of the original velocity difference



between the shearing layers. The instability condition is that the Reynolds number, $Re = LV/\nu$ with ν the viscosity, exceed some critical value.

For a sufficiently high Reynolds number the vortices originating in the instability are on their turn also susceptible to shearing instabilities, whereby a whole hierarchy of vortices, each level characterized by a length scale l and some characteristic velocity v , may develop for high Reynolds numbers. The size of the smallest eddies is set by the condition that their effective Reynolds number lv/ν should be about equal to the critical value so they can remain stable. Vortices at each level draw their energy from vortices of the next higher level by means of the instability; hence, the mechanical energy input at the largest scale L may be thought of “cascading” down to smaller and smaller scale motions until at the shortest scales it is dissipated by viscosity.

It must be emphasized that the above scenario is simplistic almost to the point of being erroneous: the series of instabilities leading to turbulence is far more complex than outlined above, and details vary greatly among flow types (Drazin and Reid, 1981). Yet this classic phenomenological picture of the origin of turbulence may be considered valid as a common denominator of the wide variety of actual processes taking place in various flows. Indeed, at this basic level it is independent of the mechanism generating the motion at the largest scales, i.e. for smaller scale turbulence it should be equally valid for turbulent convection or for random driving. At the same time one must be aware that this picture overlooks some important features of turbulence such as intermittency and coherent structures (see below).

In a more mathematical formulation, the hierarchy of “eddies” or “vortices” can be represented by a Fourier decomposition of the flow field. The wavenumber $k \sim 1/l$ then takes the place l as independent variable. The total kinetic energy of the flow may be regarded as the sum or integral of contributions from each level of the hierarchy, $E = \int E_k dk$.

Implicit in the above cascading scenario is the idea that the energy transfer is *local* in wavenumber space: each vortex draws its energy from vortices only one step higher up in the hierarchy. If the (large) energy input scale and the (small) viscous scale are separated by many orders of magnitude, one may thus expect that the local energy transfer between modes is “ignorant” of the driving processes at large scales and of the viscous processes at small scales and its dynamics is only determined by the inertial term $(\mathbf{v}\nabla)\mathbf{v}$ of the equation of motion. Hence, the shape of the spectrum in this *inertial range* cannot depend on any imposed length scale: the spectrum E_k is expected to be scale-independent, i.e. a power law. “One step” in the hierarchy then translates to one decade (or any similar fixed factor) in wavenumbers, as the vortex hierarchy is self-similar. The kinetic energy of eddies at one level is thus $v^2/2 = \int_{k/10}^k E_k dk \sim kE_k$.

2.1.2. Kolmogorov vs. Iroshnikov–Kraichnan spectra

In a stationary state where the energy input by the driving balances dissipation, the spectral energy transfer rate ϵ from low to high wavenumbers must be independent of k (and equal to the dissipation rate) in the inertial range where no significant input or dissipation occurs:

$$\epsilon \equiv v^2/2\tau = \text{const.} \quad (1)$$

where τ is the transfer timescale. In the scenario outlined above the transfer is due to the shear instabilities developing on larger eddies so its timescale is related to the growth rate of those instabilities: $\tau \sim l/v \sim (vk)^{-1}$. Substituting this into equation (1) we find $v \sim \epsilon^{1/3}k^{-1/3}$ or

$$E_k \sim \epsilon^{2/3}k^{-5/3}, \quad (2)$$

the famous Kolmogorov spectrum. There is ample evidence from experiments and observations for a Kolmogorov range in neutral fluids.

Iroshnikov (1964) and Kraichnan (1965) noted that the relation $\tau \sim l/v$ will not necessarily hold in a *conducting* fluid. In the presence of a magnetic field with an associated Alfvén speed exceeding v , the turbulent fluctuations should behave as Alfvén wave packets travelling along field lines with the Alfvén speed (the so-called Alfvénic effect). This should be the relevant case even in the absence of a large-scale mean field as the amplitude of turbulent magnetic fluctuations (produced by a small-scale dynamo, cf. Sect. 3.1) on the largest scales is high enough to dominate smaller-scale motions for all plausible spectral exponents. Iroshnikov and Kraichnan further argued that the interaction time of two wave packets of size l , travelling in the opposite direction, is $\tau_i = l/v_A \ll l/v$. In such a short time only a small amount of energy, say δE can be fed from one mode into the other. The number of such random interactions needed to change the energy of a wave packet significantly is $(E/\delta E)^2 = (v_A/v)^2$. Multiplying τ_i with this number one finds $\tau \sim (E/\delta E)^2\tau_i = (v_A/v)(l/v)$, where the Alfvén speed v_A is determined by the large-scale magnetic field, and is thus independent of l . When substituted into (1), this results in $v \sim (\epsilon v_A)^{1/4}k^{-1/4}$ or

$$E_k \sim (\epsilon v_A)^{1/2}k^{-3/2}, \quad (3)$$

known as the Iroshnikov–Kraichnan (IK) spectrum. Note that $\epsilon = \text{const.}$ implies a kinetic energy transfer rate independent of k while in the MHD case it is not the kinetic but the total (kinetic+magnetic) energy that is conserved. Similar arguments (Biskamp, 1993) can be used to show that if there is no cross-helicity the kinetic and magnetic energy spectra will be in equipartition in the inertial range, so their transfer rates are equal and constant.

In recent years doubts have arisen regarding the validity of the IK scaling in MHD turbulence. On the theoretical side, Goldreich and Sridhar (1997) pointed out some flaws in the simplified treatment of wave interactions in the IK analysis, proposing an alternative model. Politano, Pouquet, and Carbone (1998) derived exact scaling relations for certain third-order structure functions: the exponents of these scalings differ from those predicted by the IK model for similar (though not identical) correlations, suggesting (though not proving) that the IK scaling may not be correct. These findings are supported by the numerical simulations of Müller and Biskamp (1999) where instead of an IK scaling a standard Kolmogorov range was found in decaying 3D MHD turbulence with vanishing cross-helicity. The fact that the numerical values of the exponent (1.5 viz. 1.66) are quite close for the two scalings makes it difficult to distinguish between the two cases on the basis of empirical data (observations or experiments). We may thus conclude that the jury is still out on the problem of the shape of the inertial range energy spectrum in MHD turbulence. In fact, owing to departures from locality of the transfer in wave number space, the energy spectrum may not even be power law throughout (Biskamp, 1993).

2.1.3. *Inverse cascades*

As we have seen, the overall tendency is for the energy to cascade towards small scales. This is generally also true for other ideal invariants. However, if the spectra of two conserved quantities are not completely independent their simultaneous direct cascade may be inhibited so that one of them cascades towards large scales: this is known as an *inverse cascade*.

Let the spectrum H_k of a conserved quantity H be related to E_k as $H_k = h(k)k^n E_k$ where $h(k)$ has an upper or lower bound (or both). As a concrete example we may take the magnetic helicity $H = \mathbf{A}\mathbf{B}$ with \mathbf{A} the vector potential and \mathbf{B} the magnetic field strength, conserved for 3D ideal MHD turbulence; here, $n = -1$, and the relative helicity $h(k)$ is bounded from above. Taking into account equation (1), the transfer rate of H normalized by ϵ is

$$kH_k/\epsilon\tau = h(k)k^n \quad (4)$$

The constancy of this transfer rate constitutes no problem if $n < 0$ and $h(k)$ has a lower bound or $n > 0$ and $h(k)$ has an upper bound (this latter being the case for the kinetic helicity $\mathbf{u}\nabla \times \mathbf{u}$, an invariant in 3D ideal hydrodynamic turbulence). But in the case $n < 0$ with $h(k)$ bounded from above, such as in the case of magnetic helicity, the transfer rate (4) can clearly not remain constant: in the high Reynolds number limit only a vanishingly small fraction of H fed in at the input scale can be dissipated at the small scales. Most of the input of H has then no choice but to cascade towards *low* k values. Therefore, magnetic helicity suffers an inverse cascade

in 3D MHD turbulence. In fact, this inverse cascade of the magnetic helicity is responsible for the large-scale dynamo effect.

Finally, in the case if $n > 0$ and $h(k)$ is bounded from below equation (4) would predict a transfer rate *increasing* with k which, in a stationary state, is clearly an impossibility in the inertial range where no driving is present. In this situation the only way to preserve the conservation of both the energy and H is to assume $\epsilon \neq \text{const.}$ in the inertial range; instead, ϵ should decrease with k so H may show a direct cascade with a constant transfer rate there. In analogy with the previous case it is now the *energy* that must show an inverse cascade. This case is realized in 2D hydrodynamic turbulence where the enstrophy $(\nabla \times \mathbf{u})^2/2$ is an ideal invariant and its spectrum is simply $k^2 E_k$ i.e. $n = 2$ and $h(k) \equiv 1$ in this particular case.

2.1.4. Real-world turbulence vs. textbook turbulence

“Turbulence is a dangerous topic which is often at the origin of serious fights in the scientific meetings devoted to it since it represents extremely different points of view, all of which have in common their complexity, as well as an inability to solve the problem. It is even difficult to agree what exactly is the problem to be solved.”

(M. Lesieur: *Turbulence in Fluids*)

The above quote is the opening paragraph in one of the currently most widely used monographs on fluid turbulence, Lesieur (1990). It was not written having solar granulation in mind—but it could as well have been... Indeed, as we will see in the next subsection, the most debated issues are the same in the study of granulation as in other fields of turbulence: coherent structures and intermittency—those features that most strikingly distinguish turbulent flows observed in the real world from those smooth, featureless random media that one tends to envisage based on the phenomenological picture of the turbulent cascade.

In his book Lesieur suggests 3 criteria for turbulence: (1) Randomness (2) An order-of-magnitude increase in macroscopic transport, in particular in the transport of momentum¹ (3) The presence of motions on a wide and continuous range of spatial scales, spanning several decades.

The flows one tends to envisage on the basis of the above phenomenological picture of isotropic turbulence fulfil these expectations. But these criteria admit a much wider class of random flows: in fact most of the turbulent flows encountered in nature or in laboratories, while still conforming to these definitive criteria, have a strikingly different appearance from our naïve expectations. In particular, we note the ubiquitous presence of *coherent structures* and *internal intermittency*.

¹ The macroscopic diffusion coefficients in turbulence are $\sim LV$ (cf. Sect. 4). The increase in the transport of momentum then implies the usual condition $\text{Re} \equiv LV/\nu \gg 1$

Coherent structures are formations reminiscent of unstable normal modes of the instability feeding the turbulence. A classic example are coherent Kelvin-Helmholtz-like vortices in the turbulent mixing layer. What is surprising is their presence and longevity even in the regime of fully developed turbulence. Individual coherent structures are not predictable, their place and size varies with time and among different realizations of the flow. The presence and characteristics of coherent structures cannot be foreseen on the basis of spectral turbulence theory as these structures arise owing to the non-randomness of relative phases of individual Fourier modes in the flow while power spectra such as E_k contain no phase information.

The term “internal intermittency” refers to the fact that the dissipation rate is not uniformly distributed over the flow volume; instead, the dissipation is concentrated in an intermittent subset of the volume. This is sometimes somewhat vaguely formulated saying that the flow “is not everywhere turbulent”, meaning that the energy cascade reaching down to the smallest (dissipative) scales is only present in a (fractal) subset of space. Internal intermittency also modifies structure functions and spectral exponents, in particular for higher order correlations.

2.2. SOLAR OBSERVATIONS VS. THEORY

The overall properties of the solar photosphere were recently reviewed on these pages by Solanki (1998). In what follows we will focus on velocity fields only. Spatio-temporal power spectra of velocity (or intensity) fluctuations over the solar disk reveal that photospheric motions can be divided into two broad classes. (See e.g. Fig. 1 in Straus, Deubner, and Fleck, 1992.) On the high-frequency side of the line corresponding the Brunt-Väisälä frequency in the k - ω diagram one finds the familiar “ridges” corresponding to the mostly discrete spectrum of solar oscillations. On the low-frequency side of that line lies a broad continuum peaking at frequencies below 1 mHz and wavenumbers below 2 Mm^{-1} . This continuum, corresponding to granular, meso- and supergranular motions is what, guided by Lesieur’s criterion (3) above, we may tentatively identify with photospheric turbulence.

The strongest intensity contrast and the highest velocity amplitude corresponds to the characteristic cellular pattern of *granulation*, with typical spatial and temporal scales of 1 Mm and 1000 s and a velocity amplitude of 1–2 km/s. The larger scale *mesogranulation* (10 Mm, 10^4 s, 0.5–1 km/s) and *supergranulation* (30 Mm, 10^5 s, 0.3–0.5 km/s) are most easily seen in the horizontal flow pattern or in the distributions of certain tracers (magnetic flux tubes, exploding granules etc.). This suggests (despite occasional views to the contrary) that *granulation represents the energy input range of photospheric turbulence* as its strong temperature fluctuations inevitably imply strong buoyant acceleration.

2.2.1. *Is granulation turbulence?*

It must be clear from the outset that these photospheric motions must be very different from the textbook case of incompressible isotropic hydrodynamic turbulence. In particular, the scale heights of pressure and density in the photosphere are of the order of 100 km, i.e. ten times smaller than the supposed energy input range! Besides, our observations cannot resolve features below about 200 km on the solar surface; and granular observations are significantly contaminated by seeing effects already well above the formal resolution limit (Collados and Vázquez, 1987). As this resolution limit is less than a decade below the energy input scale one cannot reasonably hope to catch even a glimpse of the presumed inertial range. And yet, many observers (e.g. Espagnet *et al.*, 1993; Ruzmaikin *et al.*, 1996) try, and often claim, to fit granular power spectra by power laws or even Kolmogorov laws (ignoring not only the seeing effects and the extreme inhomogeneity but also the complete uncertainty regarding the theoretical form of the energy spectrum in 3D MHD turbulence, cf. Section 2.1.2 above).

While such efforts are clearly futile, their futility hardly warrants taking the extreme standpoint of denying the turbulent nature of granulation, as suggested recently by Nordlund *et al.* (1997). These latter authors rightly criticize the naïve attempts to fit granular power spectra by power laws, pointing out that the power spectrum of a simple step function is $\sim k^{-2}$, a power law that is hard to distinguish from the Kolmogorov law with the observational errors at hand. Cell-like granules, with their rather sharp boundaries, can also be approximately represented by a step-like function with steps of alternating sign, thereby giving rise to a power-law-like spectrum. They then nicely demonstrate that the very existence of well-defined, quasiregular granules is due to non-random relative phases of the Fourier modes of the flow. However, they then go on to suggest that this non-randomness of the phases and the corresponding semiregular, cellular pattern of the granules, their more laminar internal flow, together with the concentration of small-scale turbulence and (presumably) dissipation in the intergranular lanes are at odds with a turbulent nature of the granular flow.

Indeed —is granulation turbulence? Applying the criteria suggested by Lesieur (Sect. 2.1.4 above) we can answer affirmatively to this question. Granular motions are obviously unpredictable, and they lead to an order-of-magnitude increase in magnetic diffusivity (cf. Sect. 3 below). From the supergranular scales down to the resolution limit, a wide continuum of scales of motion is present. Small-scale turbulence, especially below the resolution limit, may indeed be concentrated in the intergranular lanes, together with dissipation (Nesis *et al.*, 1997) —but this is nothing else than the phenomenon of internal intermittency, well known from other types of turbulent flows. And as for the non-random relative phases of Fourier modes, leading to the organized, cellular appearance of granulation: this is the exact

analogue of the presence of coherent structures in other flows. Indeed, the idea I would like to promote here is that *granulae are but one example of the extensive family of coherent structures in turbulent flows*.

Whether or not we wish to call a certain flow turbulent is up to some point a merely semantic issue. But excluding a flow type from among turbulent flows just because of the presence of coherent structures and internal intermittency would amount to exclude practically all flows realized in nature, or indeed even in laboratory. Such a definition would hardly be of any practical use. In conclusion, then: granulation is a perfectly typical turbulent flow—typical even in its atypicality.

2.2.2. *The problem of the size of granules*

The characteristic granular size of ~ 1000 km presents a riddle as there is no simple explanation for the preference of such a length scale. The correlation length in deep turbulent convection is known to be approximately equal to the pressure scale height (Chan and Sofia, 1987) while in the case of granulation they differ by one order of magnitude. In the model of Antia, Chitre, and Pandey (1981) the scale is set by the scale of the most unstable normal mode in a linear stability analysis of a mixing-length model of the convective zone, taking into account turbulent heat transfer. The resulting scale is indeed in reasonable agreement with granular sizes.

An alternative explanation was proposed recently by Rast (1999). In his scenario the basic units are not the granules but the downflow plumes in between, initiated by localized cooling events. In 2D numerical experiments in an adiabatic layer he finds that if the separation of two neighbouring plumes exceeds a certain limit, a new starting plume spontaneously forms in between. The relation of this result to the existence of two granule populations (Hirzberger *et al.*, 1997) is unclear but the mechanism suggested by Rast, coupled with the supposed coalescence of plumes getting too close, could regulate the mean separation between plumes. It remains to be seen whether such a scenario can also reproduce granule sizes quantitatively, in a realistic, 3D model.

2.2.3. *The origin of supergranulation*

If the energy deposited at the granular scales cascades towards the smaller scales, to be ultimately dissipated in the intergranular lanes, what is the origin of larger scale velocity fields such as meso- and supergranulation? Maybe the oldest answer to this question is that they may be the surface imprint of larger scale convective motions taking place in deeper layers where the pressure scale height is much larger. In their work cited above, Antia, Chitre, and Pandey (1981) found a second peak in the growth rate-wavenumber relation of normal modes. The scale of this peak, 10–20 Mm, invites identification with supergranulation.

Another suggestion was made by Krishan (1991) who proposed that supergranulation is due to some kind of inverse cascade taking place in the photosphere. The particular cascade she proposed involved the mean square kinetic helicity—an ideal invariant in 3D hydrodynamic turbulence.

Supergranulation is best seen in the distribution of network magnetic fields, leading to the suggestion that the magnetic field itself may have a crucial role in the origin of the flow pattern (Zwaan, private comm.). This scenario may possibly be combined with an inverse-cascade-type model recalling that in 3D MHD turbulence magnetic helicity suffers an inverse cascade.

As we see, possibilities abound but none has been pursued to the point of giving testable predictions. The problem of the origin of supergranulation is as open as it was three decades ago, at the time of its discovery.

3. The Turbulent Magnetic Field

3.1. α -EFFECT AND SMALL-SCALE DYNAMO

Beside the fluctuating velocity field, magnetic fields also have a fluctuating component in a turbulent plasma. While a strong large-scale field will obviously contribute to small-scale fluctuations, a turbulent magnetic field of significant strength is present in 3D MHD turbulence even in the absence of a global field. This field is generated by small-scale dynamo action.

Dynamo effects come in two varieties. *Large-scale* dynamos involve the growth/maintenance of an organized, large-scale (as compared to the integral scale of turbulence) mean magnetic field. As we already mentioned, large-scale dynamo effect is intimately linked to the inverse cascade of magnetic helicity in 3D MHD turbulence. The best known of these effects is the α -effect, consisting of the appearance of a mean electromotive force proportional to the mean field strength: $\vec{\mathcal{E}} = \alpha \langle \mathbf{B} \rangle$. α is a pseudoscalar, so for this effect to appear, the flow should violate parity invariance.

In *small-scale* dynamos, in contrast, no mean magnetic field is generated; yet, the mean magnetic energy density $\langle B^2 \rangle / 2\mu$ and the unsigned flux density $\langle |\mathbf{B}| \rangle$, grow exponentially (kinematical case) or are maintained (hydromagnetic case). This effect can also occur in parity invariant flows.

Consider the most widely known (though by no means the only) physical mechanism capable of maintaining a dynamo: helical flows. A localized helical flow acts a stretch-twist-fold type dynamo on a preexisting weak large-scale field. The resulting field configuration can be regarded as the superposition of a closed flux ring and the original weak field (on which the whole process can be infinitely repeated). Whether the closed loop is actually detached from the preexisting field by reconnection or this is just

a convenient mathematical decomposition, is irrelevant. The orientation of the ring depends on the sign of the helicity in the original flow. If the mean helicity is zero (mirror symmetry) the resulting loops will be randomly oriented and their field will cancel on the mean, i.e. no mean magnetic field is produced. Their magnetic energy density however does not cancel so we are dealing with a small-scale dynamo. If, on the other hand, there is a preferred sense of rotation in the flow (mean helicity does not vanish) the loops will show a preferred orientation thus giving rise to a net large-scale field: this is the case of the large-scale dynamo.

The condition for these effects to work in a flow is in general a sufficiently high magnetic Reynolds number LV/ν_m where ν_m is the (molecular) magnetic diffusivity. This condition is fulfilled in the solar photosphere, so it has been suggested by several authors (Petrovay and Szakály, 1993; Cattaneo, 1999) that a small-scale dynamo is operative there. (Mean helicity is negligible in the photosphere so large-scale dynamo effect is absent.)

What is the saturated state of the small-scale dynamo? Numerical experiments and turbulence closure models (e.g. De Young, 1980; Meneguzzi and Pouquet, 1989; Cattaneo, 1999; Subramanian, 1999) invariably show that in high Reynolds number driven non-helical MHD turbulence, especially in flows of convective origin,

- magnetic energy density saturates at a value about an order of magnitude below kinetic energy density
- magnetic field structure is extremely intermittent; the strongest structures (tubes) have a magnetic energy density comparable to the kinetic energy density; the typical tube filling factor is thus $f \sim 0.1$. The analytic result of Subramanian (1999) predicts $f = 0.025 TV/L$, T being the correlation time.
- the magnetic energy spectrum peaks at significantly higher wavenumbers than the kinetic energy spectrum.

An issue that has given rise to much controversy in recent years has been the claimed strong suppression of the α -effect by even a very weak magnetic field (see e.g. Section 4 of Petrovay and Zsargó, 1998, for a summary of the argument). Here I would just like to call attention to the little appreciated fact that if a suppression of α does take place then it should also affect the small-scale dynamo, given that the underlying physical mechanisms are the same. While the large-scale dynamo may be salvaged by other non-classical α -mechanisms, this may be much more difficult for the small-scale dynamo. And yet, as we said, small-scale dynamo action undeniably exists and is extremely common in turbulent MHD simulations. This puzzle is not just unsolved but rarely even recognized.

On the basis of what was said above one may expect that the photospheric turbulent field should be characterized by a mean unsigned flux

density that is crudely an order of magnitude lower than the photospheric equipartition field strength (400 G), and its characteristic scale (correlation length) should be about 100 km, well below the resolution limit. How can we hope to observe this mixed-polarity field?

3.2. HANLE DIAGNOSTICS OF THE TURBULENT MAGNETIC FIELD

The Zeeman effect, our traditional diagnostic tool for solar magnetism, is “blind” to fields with polarities mixed on scales below the resolution limit. In such a field the net magnetic flux in a pixel most of the time remains below the resolution limit, and only occasionally, thanks to statistical fluctuations, can one expect to detect a weak signal of random polarity. This Zeeman-detectable part of the turbulent field, the so-called *intranetwork field* is however but the tip of the iceberg, and most of the turbulent field remains undetected.

An alternative detection method is offered by the *Hanle effect*. This effect consists in a reduction of the linear polarization of coherently scattered light if the scattering occurs in a magnetic field (Stenflo, 1994). The use of this method for the detection of solar turbulent fields has come to its own in the last decade (Faurobert-Scholl, 1993; Bianda, Stenflo, and Solanki, 1998, etc.). The increased interest in a rigorous interpretation of scattering line polarization observations has motivated the development of very efficient numerical methods for the transfer of polarized radiation and Hanle-effect codes (Trujillo Bueno and Manso Sainz, 1999). The consensus now seems to be that at the height of line formation the turbulent flux density is $\sim 10\text{-}20$ G; however, many controversies still remain, such as the “Na solar paradox” (Landi Degl’Innocenti, 1998). For a critical discussion on this point, with an advance of some interesting new results see Trujillo Bueno (1999).

One of the most intriguing recent discoveries is the finding of Stenflo, Keller, and Gandorfer (1998) that the degree of linear polarization Q/I shows large amplitude random variations over the solar disk. A phenomenological model for the origin of such fluctuations (Petrovay, 1999) suggests that they may be interpreted rather naturally on the basis of statistical fluctuations of the small-scale dynamo mechanism.

4. Turbulent magnetic diffusion

4.1. RANDOM WALK AND BABCOCK-LEIGHTON MODELS

The random horizontal flow on the solar surface leads to a random motion of tracers, the most important of which are magnetic flux tubes. A simple random walk of stepsize Δx and timestep Δt over a plane is known to lead

to an increase of the rms separation r of a tracer from its starting point (or of two tracers from each other) according to the law

$$r^2 = 4Dt \quad (5)$$

where $D = \Delta x^2/2\Delta t$. The time development of a continuous distribution of tracers is then described by a diffusion equation with diffusivity D .

As a first approximation, the advection of tracers by (super)granules may be represented by such a simple random walk/diffusion, identifying Δx with the spatial scale l of the cells and Δt with their lifetime τ .

This is the approach used in Babcock–Leighton-type models of the solar cycle where poloidal fields are brought to the surface in a concentrated form in active regions, and thereafter they are passively transported to the poles by transport processes (diffusion and meridional circulation). The diffusivity in these models is a free parameter: a best fit to the observations yields $D = 600 \text{ km}^2/\text{s}$. Despite the vectorial character of the magnetic field, these 1D models have been remarkably successful in reproducing the observed temporal evolution of the flux distribution. A possible explanation was proposed in their model by Wang, Sheeley, and Nash (1991): they assume that field lines are vertically oriented throughout much of the convective zone and this essentially reduces the problem to one dimension. Some support for this conjecture has come from the 2D flux transport models of Petrovay and Szakály (1999). Thus, in a first approximation, 1D models may be used for the description of meridional transport, as these fields pervade the convective zone and are continuously reprocessed through it.

The empirically determined value of the diffusivity, $600 \text{ km}^2/\text{s}$, seems to agree with the primitive random walk model if the steps are identified with granular sizes/lifetimes. Supergranulation, however, should lead to a diffusivity that is by an order of magnitude higher than this calibration. The continuous reprocessing of large-scale fields throughout the convective zone offers a plausible explanation for this inconsistency: the empirical value of the diffusivity reflects the turbulent diffusivity in the lower convective zone where the pressure scale height is $\sim 50 \text{ Mm}$ and the turnover time $\sim 1 \text{ month}$.

An alternative explanation was put forward by Ruzmaikin and Molchanov (1997) who pointed out that, owing to the cellular nature of photospheric flows, identifying cell size l and lifetime τ with random walk steps is an oversimplification. The fact that a tracer cannot leave a cell during the cell's lifetime, even if it was originally placed next to its border, reduces the effective stepsize significantly. The resulting reduction in D is very sensitive to the value of the Strouhal number $\text{St} = \tau v/l$ and is especially strong for $\text{St} \gg 1$. This effect may be sufficient to reduce supergranular diffusivity to the observed value.

4.2. ANOMALOUS DIFFUSION

The cellular and turbulent nature of the flow implies that a simple random walk cannot account for the motion of magnetic elements. As a consequence, the actual flux redistribution may differ from a simple (Fickian) diffusion process (Isichenko, 1992) and, instead of equation (5) in general one has

$$r = 2Kt^\zeta. \quad (6)$$

If $\zeta \neq 1/2$ it is customary to speak of *anomalous* or *non-Fickian diffusion*, $\zeta > 1/2$ corresponding to *superdiffusion*, $\zeta < 1/2$ to *subdiffusion*. As equation (6) means a unique relation between r and t one might formally still write $r = 2K'(r)t^{1/2}$, leading to the concept of a “scale-dependent diffusivity”

$$D(r) = K'^2 = K^{1/\zeta} r^{2-1/\zeta} \quad (7)$$

It is however clear that such a concept is in general useless for the description of the evolution of a continuous field where no preferred scale exists. Anomalous diffusion thus cannot be described by a diffusion equation or, indeed, by any partial differential equation.

How can anomalous diffusion come about? One possibility was suggested by Schrijver and Martin (1990). Magnetic flux tubes are located at junctions of a fractal lattice between supergranules, mesogranules and granules. Assuming that limitations exist for the motion of individual flux elements along this lattice, for certain lattice properties subdiffusion may result. They made an attempt to detect subdiffusion by the analysis of observed flux redistribution in the photosphere; however, ζ was not found to differ from 0.5 within the observational uncertainties.

Being a multiscale phenomenon, turbulence can also naturally lead to a “scale-dependent diffusivity”. In order to understand the nature of the diffusion process in a turbulent medium let us consider the question how a random continuous velocity field of a given characteristic scale λ (i.e. one level in the turbulent hierarchy) can be best represented by a random walk with steps Δx and Δt . For the best representation one should set $\Delta t = \tau_L$, the Lagrangian correlation time of the flow, as this is just the time after which the advected particle experiences a significant change in its velocity. The distance the particle travels in this time is $\Delta x = v\tau_L = \min(v\tau_E, \lambda)$ where τ_E is the Eulerian correlation time, λ the correlation length, and v the rms velocity. The diffusivity for this random walk will thus depend on the Strouhal number $St = \tau_E v / \lambda$; assuming a non-cellular flow

$$D = \begin{cases} \tau_E v^2 & \text{if } St < 1 \\ \lambda v & \text{if } St > 1 \end{cases} \quad (8)$$

In a multiscale flow both τ_E and v scale with λ :

$$\tau_E \sim \lambda^z \quad v^2 \sim \lambda^{\alpha-1} \quad (9)$$

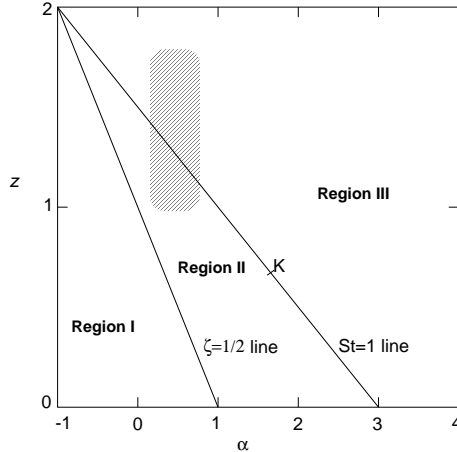


Figure 1. Regimes of anomalous diffusion on the α - z plane. K is the Kolmogorov point; the shaded area indicates the approximate position of the photospheric flow field in the 1–30 Mm size range. (Non-cellular case)

During the random walk, motions on scales exceeding the separation r of two tracers do not contribute to their further separation while all other scales contribute to it. Of these scales, according to equation (7), the smallest one will dominate in the diffusion process for $2 - 1/\zeta < 1$ i.e. $\zeta < 1/2$. In this case, then, the diffusivity will not significantly depend on the separation for all scales above the viscous scale: turbulence can never lead to subdiffusion.

In the case when the relatively largest scale $\lambda \sim r$ dominates, for given values of z and α the anomalous diffusion exponent ζ can be determined by substituting (9) into (8) and equating the resulting scaling exponent of D to $2 - 1/\zeta$, as given by (7). The Strouhal number scales as $St \sim \lambda^{z+\alpha/2-3/2}$. For high Reynolds numbers, then, the sign of $(St - 1)$ at the larger scales depends on the sign of the scaling exponent of St , i.e. the line

$$2z + \alpha - 3 = 0 \quad (10)$$

defines two regimes in the α - z plane (Fig. 1). Above the line, in what is called Region III (Avellaneda and Majda, 1992), one finds $\zeta = 2/(3 - \alpha)$ (except in the case of a cellular flow when $\zeta = 1/z$ —cf. the discussion at the end of Sect. 4.1). This Region is clearly superdiffusive for all values of $\alpha > -1$ (or $z < 2$). Below the line, in Region II we have $\zeta = 1/(3 - z - \alpha)$, independent of cellularity, as here we have low Strouhal numbers at the large scales. It is then clear that a second dividing line will also exist at

$$z + \alpha = 1 \quad (11)$$

as below that line (Region I) $\zeta < 1/2$ would result, in which case, as we have seen, the smallest scales dominate the diffusion process. Region I is thus

characterized by a Fickian diffusion, while Region II is again superdiffusive. Point K in Figure 1 denotes the case of a Kolmogorov spectrum, $\alpha = 5/3$, $z = 2/3$, $\zeta = 3/2$.

In order to determine the place of photospheric velocity fields on the α – z diagram, Ruzmaikin *et al.* (1996) fitted power laws to the spatio-temporal power spectra of photospheric velocity fields with the result $\alpha \sim 1.5$ – 1.8 , $z \sim 0.15$ – 0.85 . This would localize solar turbulence to the neighbourhood of the Kolmogorov point K . However, in Section 2.2.1 above we already stressed the perils of power-law fits to power spectra of solar velocity fields. There is simply no theoretical reason or observational evidence to suggest that these fields should follow a power-law spectrum from supergranular scales down to the resolution limit. Indeed, the well known fact that meso- and supergranular motions have a lower velocity amplitude than granulation, tells us that $\alpha < 1$ in the regime $\lambda > 1$ Mm! Using observational estimates for these velocity amplitudes and for correlation times one arrives at much more robust limits that are in plain contradiction to the ones quoted above: $\alpha \sim 0.0$ – 0.7 , $z \sim 0.9$ – 1.8 , leading to $\zeta \sim 0.48$ – 1.2 . These limits in themselves would indicate superdiffusion (shaded area in Fig. 1).

Turbulent erosion models of sunspot decay can also be used to constrain anomalous diffusion in the photosphere (Petrovay, 1998). The size of sunspots spans the granular-supergranular size range that is of interest in this respect, and the fortuitous property of the erosion models that they *do* show a characteristic scale, the radius of the spontaneously formed current sheet, makes it possible to test for ζ by using a scale-dependent diffusion coefficient with the current sheet radius as defining scale. In this way, ζ is found to lie in the range 0.44–0.59, i.e. any deviation from a Fickian diffusion seems to be modest, if present at all. A possible explanation for why the diffusion exponent is lower than suggested by velocity power spectra may be that superdiffusion due to turbulence is offset by subdiffusion effects due to diffusion on a bond lattice.

Acknowledgements

This work was funded by the DGES project no. 95-0028, the FKFP project no. 0201/97, and the OTKA project no. T032462.

References

Antia, H. M., Chitre, S. M., and Pandey, S. K.: 1981, *Solar Phys.* **70**, 67
 Avellaneda, M. and Majda, A. J.: 1992, *Phys. Fluids A* **4**, 41
 Bianda, M., Stenflo, J. O., and Solanki, S. K.: 1998, *Astron. Astrophys.* **337**, 565
 Biskamp, D.: 1993, *Nonlinear Magnetohydrodynamics*, Cambridge UP, Cambridge

Cattaneo, F.: 1999, *Astrophys. J.* **515**, L39

Chan, K. L. and Sofia, S.: 1987, *Science* **235**, 465

Collados, M. and Vázquez, M.: 1987, *Astron. Astrophys.* **180**, 223

De Young, D. S.: 1980, *Astrophys. J.* **241**, 81

Drazin, P. G. and Reid, W. H.: 1981, *Hydrodynamic Stability*, Cambridge UP, Cambridge

Espagnet, O., Muller, R., Roudier, T., and Mein, N.: 1993, *Astron. Astrophys.* **271**, 589

Faurobert-Scholl, M.: 1993, *Astron. Astrophys.* **268**, 765

Goldreich, P. and Sridhar, S.: 1997, *Astrophys. J.* **485**, 680

Hirzberger, J., Vázquez, M., Bonet, J. A., Hanslmeier, A., and Sobotka, M.: 1997, *Astrophys. J.* **480**, 406

Iroshnikov, P. S.: 1964, *Sov. Astron.* **7**, 566

Isichenko, M. B.: 1992, *Rev. Mod. Phys.* **64**, 961

Kraichnan, R. H.: 1965, *Phys. Fluids* **10**, 1417

Krishan, V.: 1991, *Monthly Notices Roy. Astron. Soc.* **250**, 50

Landi Degl'Innocenti, E.: 1998, *Nature* **392**, 256

Lesieur, M.: 1990, *Turbulence in Fluids*, 2nd ed., Kluwer, Dordrecht

Meneguzzi, M. and Pouquet, A.: 1989, *J. Fluid Mech.* **205**, 897

Müller, W.-C. and Biskamp, D.: 1999, *arXiv:physics/9906003*

Nesis, A., Hammer, R., Hanslmeier, A., Schleicher, H., Sigwarth, M., and Steiger, J.: 1997, *Astron. Astrophys.* **326**, 851

Nordlund, Å., Spruit, H. C., Ludwig, H.-G., and Trampedach, R.: 1997, *Astron. Astrophys.* **328**, 229

Petrovay, K.: 1998, in E. R. Priest, F. Moreno-Insertis, and R. A. Harris (eds.), *A crossroads for european solar and heliospheric physics: recent achievements and future mission possibilities*, ESA, Publ. SP-417, p. 273

Petrovay, K.: 1999, in T. R. Rimmele, K. S. Balasubramaniam, and R. R. Radick (eds.), *High Resolution Solar Physics: Theory, Observations, and Techniques*, Proc. 19th Sac Peak Workshop, ASP Conf. Series **183**, San Francisco, p. 70

Petrovay, K. and Szakály, G.: 1993, *Astron. Astrophys.* **274**, 543

Petrovay, K. and Szakály, G.: 1999, *Solar Phys.* **185**, 1

Petrovay, K. and Zsargó, J.: 1998, *Monthly Notices Roy. Astron. Soc.* **296**, 245

Politano, H., Pouquet, A., and Carbone, V.: 1998, *Europhys. Lett.* **43**, 516

Rast, M.: 1999, in T. R. Rimmele, K. S. Balasubramaniam, and R. R. Radick (eds.), *High Resolution Solar Physics: Theory, Observations, and Techniques*, Proc. 19th Sac Peak Workshop, ASP Conf. Series **183**, San Francisco, p. 443

Ruzmaikin, A. A., Cadavid, A. C., Chapman, G. A., Lawrence, J. K., and Walton, S. R.: 1996, *Astrophys. J.* **471**, 1022

Ruzmaikin, A. A. and Molchanov, S. A.: 1997, *Solar Phys.* **173**, 223

Schrijver, C. J. and Martin, S. F.: 1990, *Solar Phys.* **129**, 95

Solanki, S.: 1998, *Space Sci. Rev.* **85**, 175

Stenflo, J. O.: 1994, *Solar Magnetic Fields: Polarized Radiation Diagnostics*, Kluwer, Dordrecht

Stenflo, J. O., Keller, C. U., and Gandorfer, A.: 1998, *Astron. Astrophys.* **329**, 319

Straus, T., Deubner, F.-L., and Fleck, B.: 1992, *Astron. Astrophys.* **256**, 652

Subramanian, K.: 1999, *Phys. Rev. Lett.* **83**, 2957

Trujillo Bueno, J.: 1999, in K. N. Nagendra and J. O. Stenflo (eds.), *Solar Polarization*, Proc. Bangalore conference, Kluwer, San Francisco, p. 73

Trujillo Bueno, J. and Manso Sainz, R.: 1999, *Astrophys. J.* **516**, 436

Wang, Y.-M., Sheeley, N. R., and Nash, A. G.: 1991, *Astrophys. J.* **383**, 431